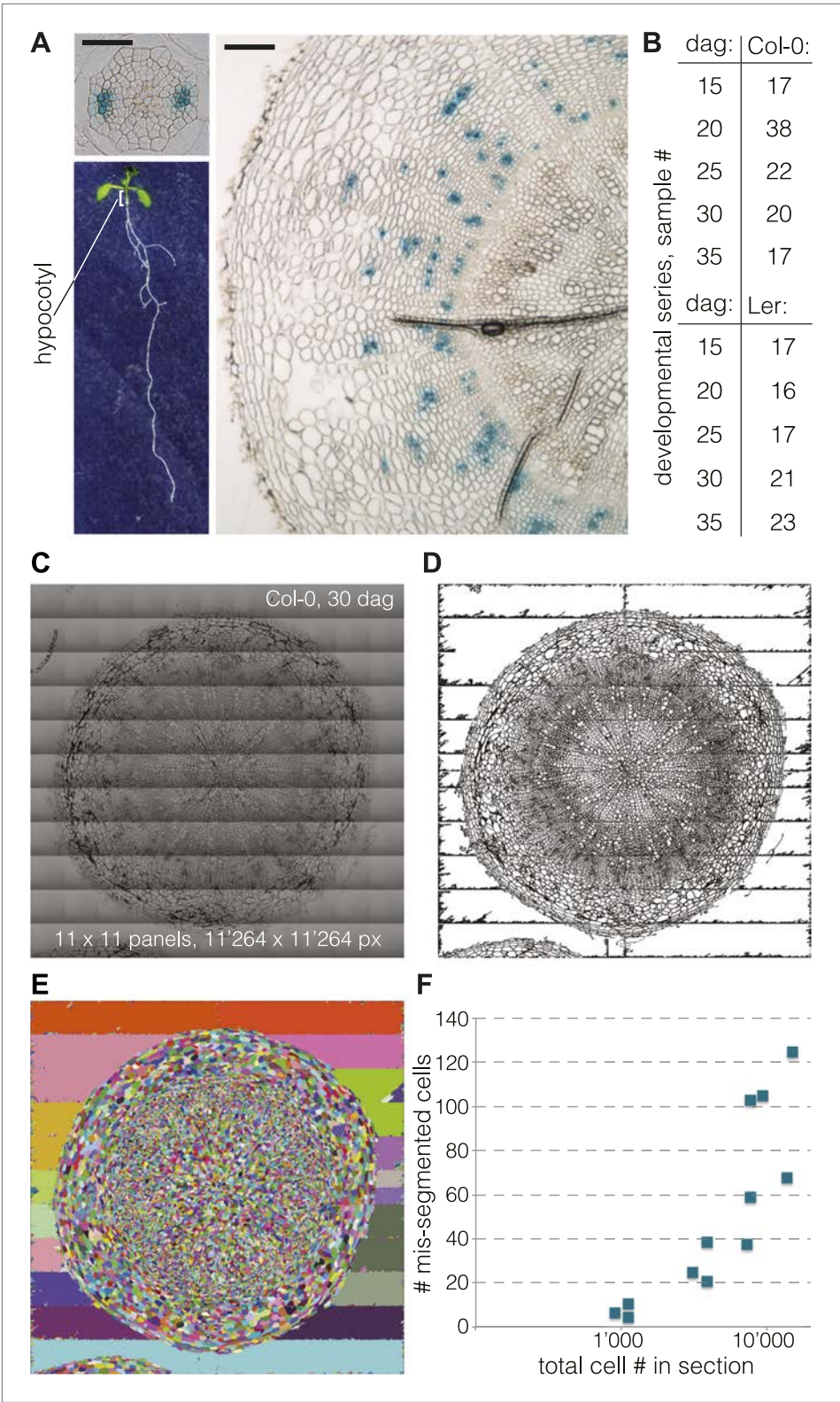


---

## Figures and figure supplements

Automated quantitative histology reveals vascular morphodynamics during  
Arabidopsis hypocotyl secondary growth

**Martial Sankar, et al.**



**Figure 1.** Cellular level analysis of Arabidopsis hypocotyl secondary growth. **(A)** Light microscopy of cross sections obtained from Arabidopsis hypocotyls (organ position illustrated for a 9-day-old seedling, lower left) at 9 dag (upper left) and 35 dag (right). Size bars are 100  $\mu$ m. Blue GUS staining due to the presence of an *APL::GUS* reporter gene in this Col-0 background line marks phloem bundles. **(B)** Overview of the developmental series

Figure 1. Continued on next page

Figure 1. Continued  
(time points and distinct samples per genotype) analyzed in this study. (C) Example of a high-resolution hypocotyl section image assembled from 11 × 11 tiles. (D) The same image after pre-processing and binarization, and (E) subsequent segmentation using a watershed algorithm. (F) Number of mis-segmented cells as determined by careful visual inspection in 12 sections, plotted against the total number of cells per section (log scale).  
DOI: 10.7554/eLife.01567.003

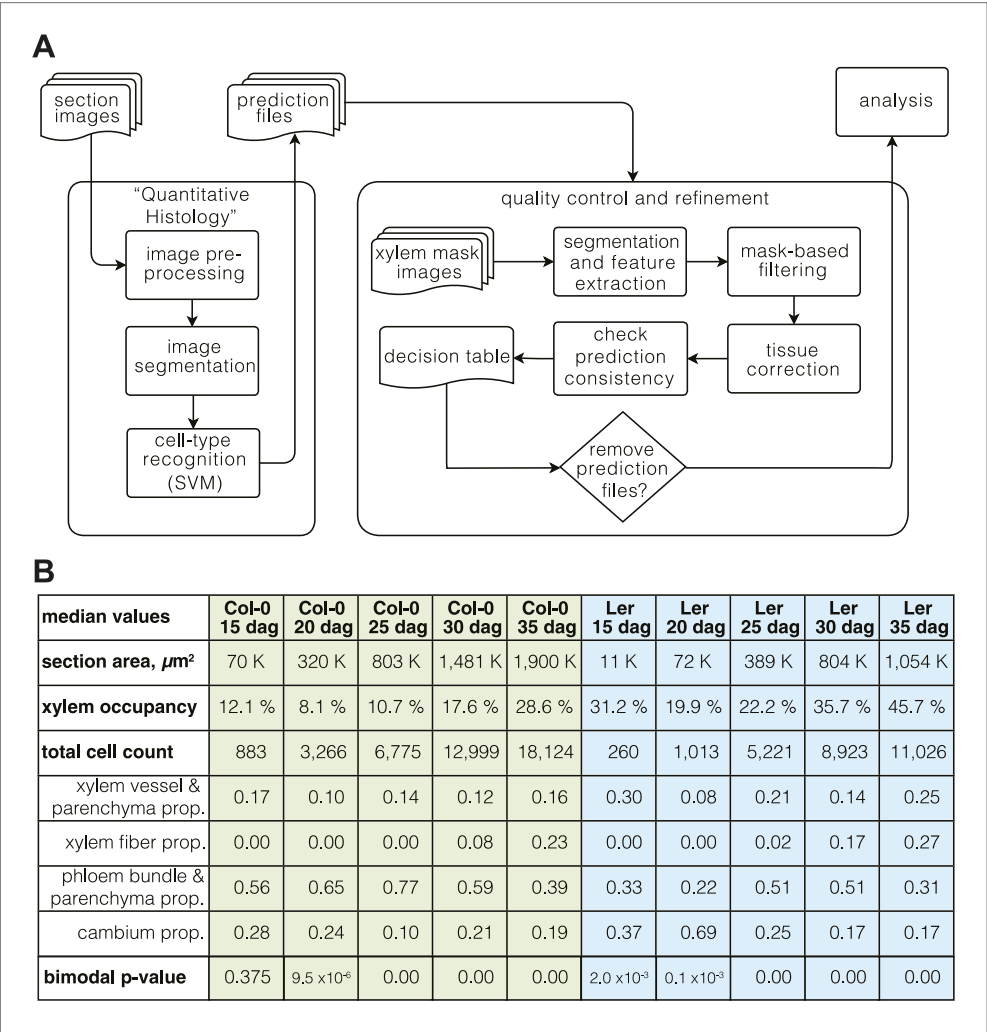
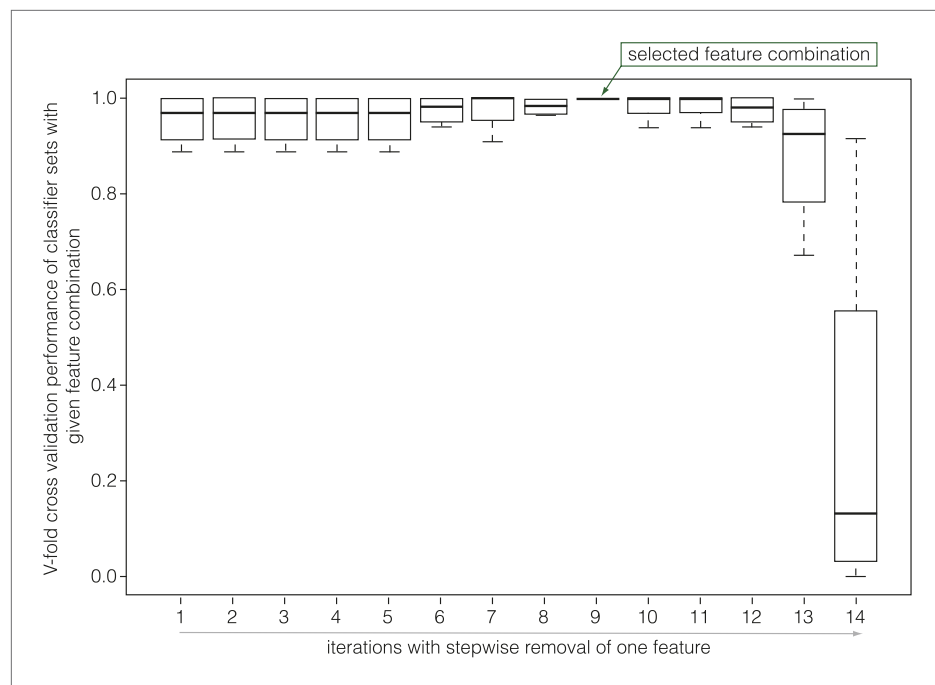
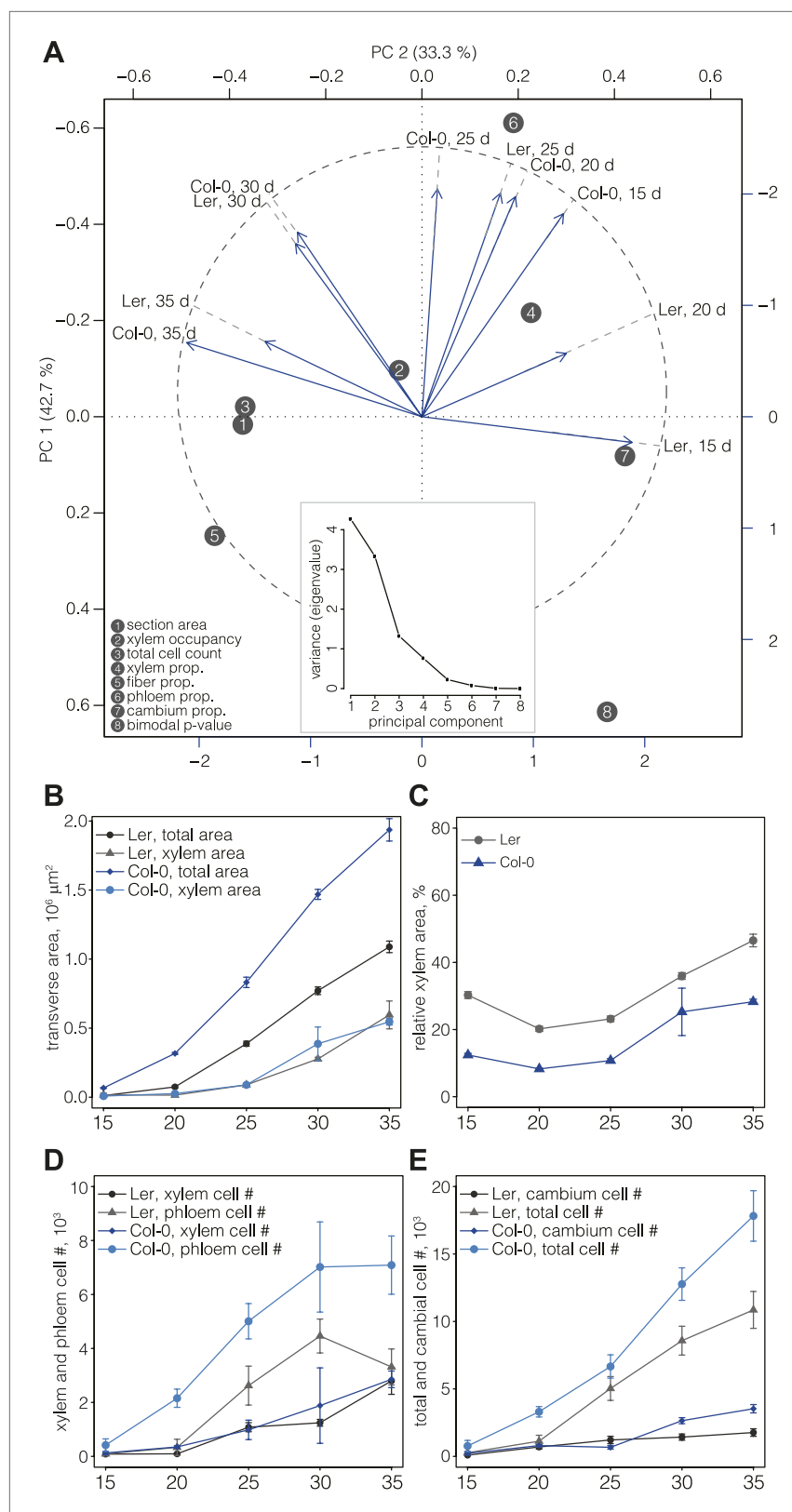


Figure 2. The ‘Quantitative Histology’ approach. (A) Overview of the computational pipeline from image acquisition to analysis. (B) ‘Phenoprints’ for the different genotypes and developmental stages.  
DOI: 10.7554/eLife.01567.004



**Figure 2—figure supplement 1.** An example of classifier selection through V-fold cross validation.

DOI: [10.7554/eLife.01567.005](https://doi.org/10.7554/eLife.01567.005)



**Figure 3.** Progression of tissue proliferation. **(A)** Principal component analysis (PCA) of the phenoprints shown in **Figure 2B**, performed with normalized values (**Supplementary file 4**). The inset screeplot displays the proportion of total variation explained by each principal component. **(B–E)** Comparative plots of parameter progression in the **Figure 3**. *Continued on next page*

Figure 3. Continued

two genotypes. In (D), xylem represents combined vessel, parenchyma, and fiber cells, phloem represents combined phloem parenchyma and bundle cells. Error bars indicate standard error.

DOI: [10.7554/eLife.01567.006](https://doi.org/10.7554/eLife.01567.006)

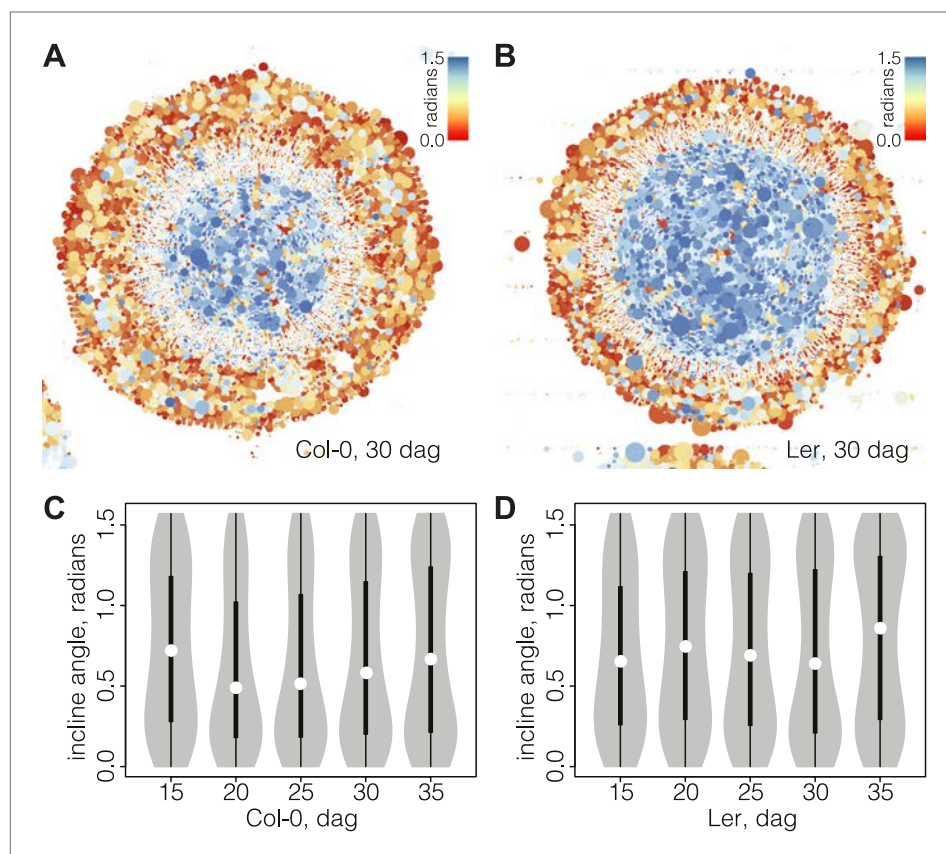


**Figure 4.** Bimodal distribution of incline angle according to position. (A and B) Spatial distribution of cell incline angle illustrates the vascular organization in Ler (B) as compared to Col-0 (A) at later stages of development, for example 30 dag. The size of the disc increases with the area of the cell. Blue color indicates radial cell orientation, red orthoradial. (C and D) Violin plots of incline angle distribution, illustrating increasingly bimodal distribution coincident with refined vascular organization and different dynamics of the process in the two genotypes.

DOI: [10.7554/eLife.01567.007](https://doi.org/10.7554/eLife.01567.007)

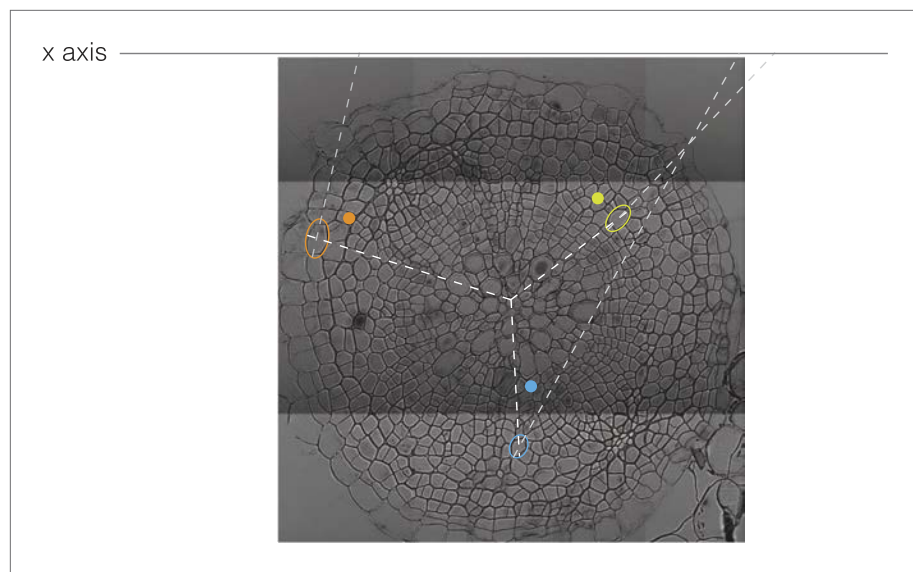


**Figure 4—figure supplement 1.** An illustration of the incline angle.

DOI: [10.7554/eLife.01567.008](https://doi.org/10.7554/eLife.01567.008)



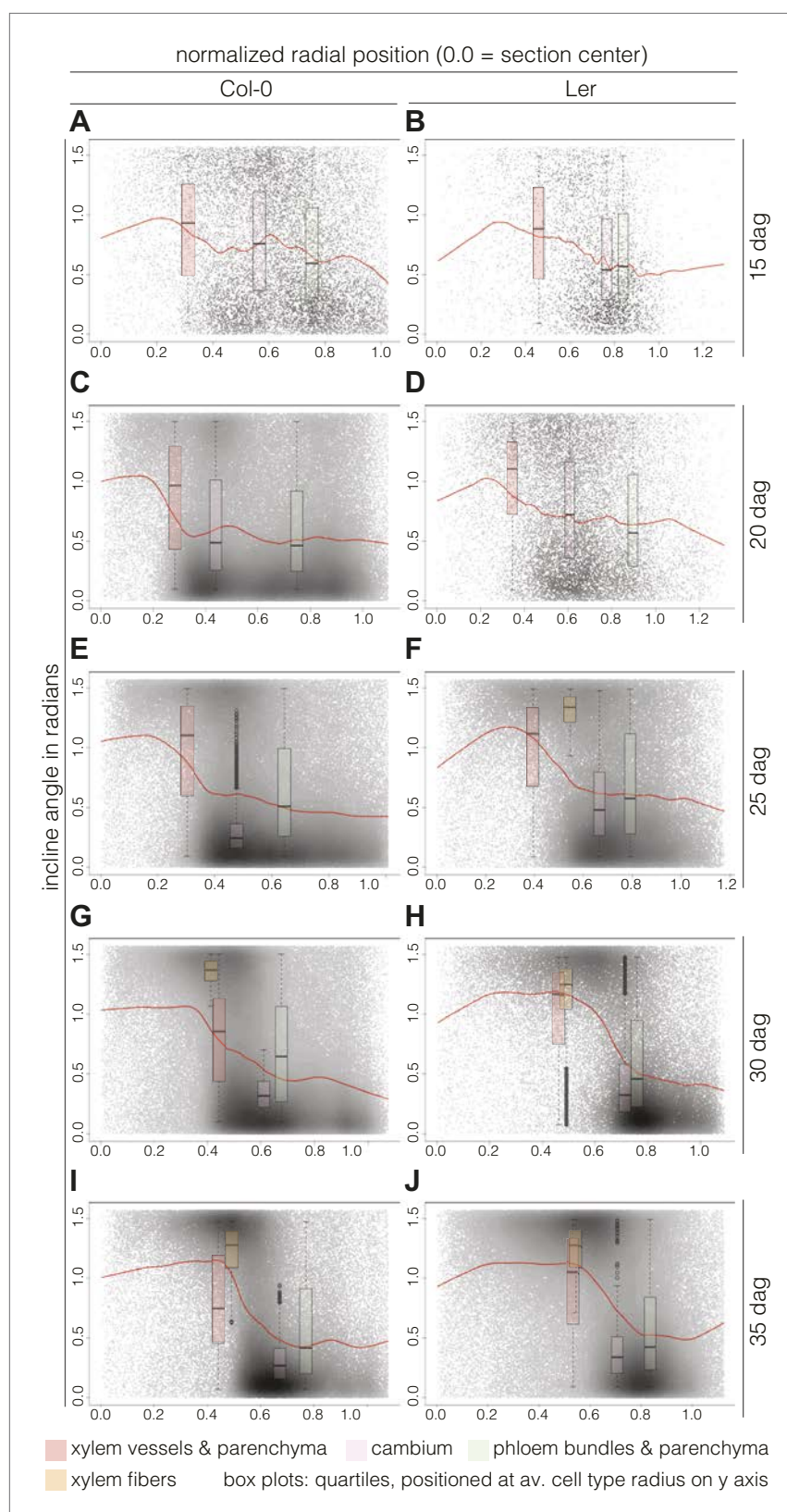


**Figure 5.** Distinct local organization of incline angle during hypocotyl secondary growth progression. (A–J) Density plots of cell incline angle vs radial position for the two genotypes at the indicated developmental stages, representing all cells across all sections for a given time point. The red lines represent the fit of these cloud distributions

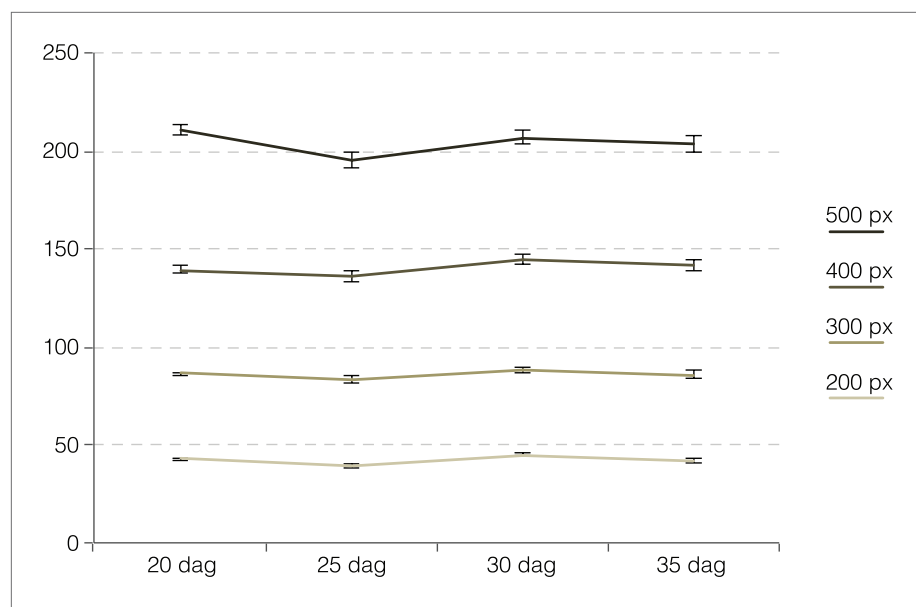
Figure 5. Continued on next page



Figure 5. Continued

with locally weighted linear regression (i.e., lowess), revealing the essential data trends. All sections were normalized from 0.0 (the manually defined center) to 1.0 (the average radius in a set of sections as determined by the average distance of the outermost cells from the center for individual sections). Box plots indicate the quartiles of the radian distribution for each cell-type class and are placed at the average position of the cell type with respect to the y axis. Outliers are shown as circles.

DOI: [10.7554/eLife.01567.009](https://doi.org/10.7554/eLife.01567.009)



**Figure 5—figure supplement 1.** Analysis of cell number in defined xylem regions of different size.

DOI: [10.7554/eLife.01567.010](https://doi.org/10.7554/eLife.01567.010)

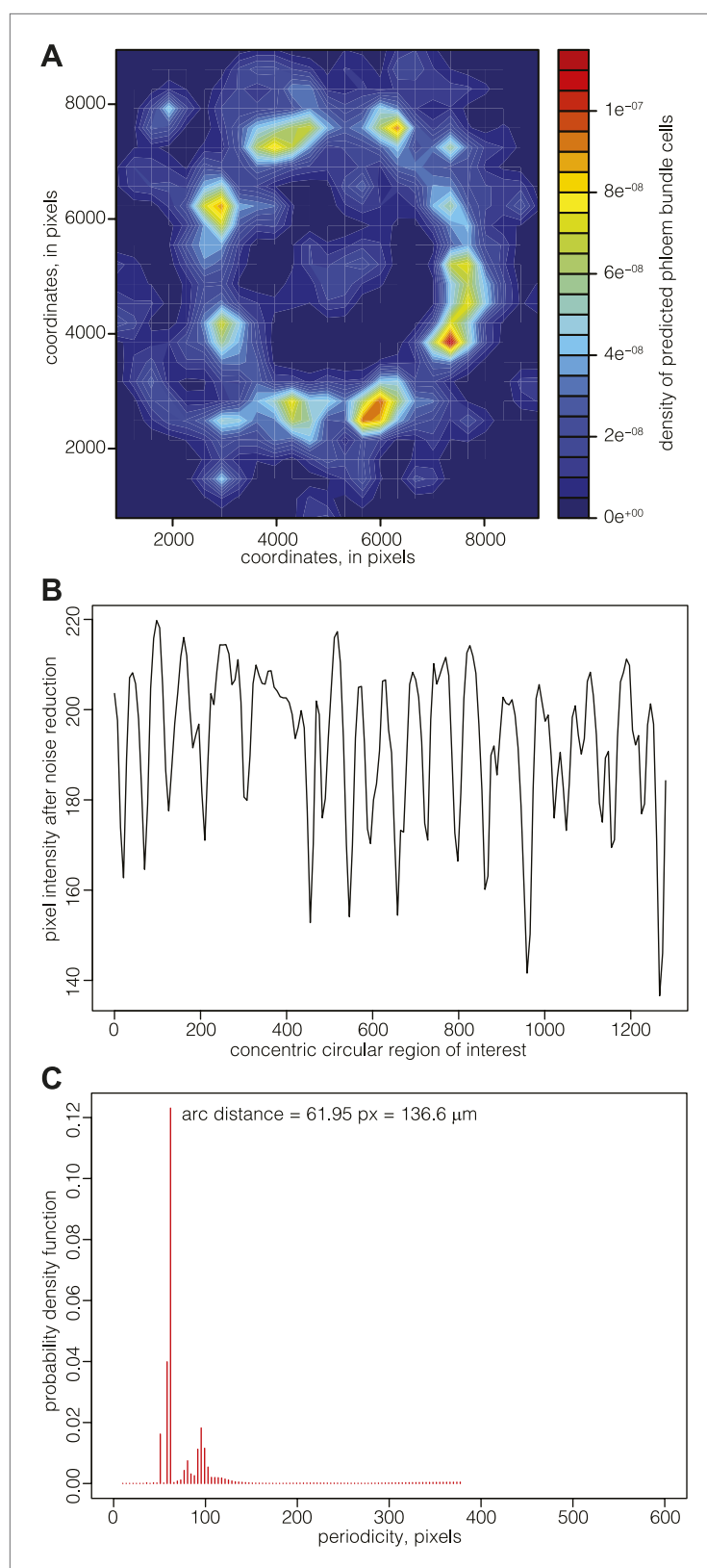


**Figure 6.** Mapping of phloem pole patterning. **(A)** Example of Gaussian kernel density estimate of the location of predicted phloem bundles cells in a 30 dag Col-0 section. High density represents phloem poles. **(B)** Example of an analysis of emerging phloem pole position in a 30 dag Col-0 section. The plot represents a pixel intensity map after noise reduction. **(C)** Example of a probability density function of periodicity in pixels. The plot represents a pixel intensity map after noise reduction. *Figure 6. Continued on next page*

*Figure 6. Continued*

noise reduction along a circular region of interest across the emerging phloem poles. Intensity peaks are due to GUS staining conferred to phloem bundles by an *APL::GUS* reporter construct. **(C)** Probability density function of the data shown in **(B)** obtained from an automated Bayesian model. The dominant single peak indicates a constant arc distance of ca. 62 pixel between the phloem poles.

DOI: [10.7554/eLife.01567.011](https://doi.org/10.7554/eLife.01567.011)